

# Energy Absorption of Axially-Impacted Column Controlled by Transverse Impact

Tadaharu Adachi

**Abstract** Energy absorption of a column under an axial impact was controlled by a transverse impact which attributed instantaneous reduction of the structural stiffness. It was found that the absorption of the axial impact energy increased due to the post-buckling deformation being enlarged by transverse impact, though the axial impact load decreased. The experiment showed that the time elapsed from the beginning of the axial impact to the transverse impact significantly influenced the energy absorption. A transverse impact applied simultaneously with an axial impact produced the highest energy absorption. The method suggested in this paper could increase the energy absorption without losing any stiffness and static strength.

## 1 Introduction

Safety is becoming a vital issue in the design of modern transportation means such a vehicle, train, helicopter and airplane. In recent years, impact energy absorption during structural crash becomes very important and is excessively investigated. Generally, in a collision, the structure collapses within the crushable zone to absorb the impact energy for safety of the passenger [1-3]. The most common method to easily collapse a structure is reducing its structural stiffness by adding imperfections such as dents and bents [4,5].

However, this method has a consequence of reducing the stiffness which is very important for a better operation performance, minimizing vibration and noise. Therefore, it is important to maintain high stiffness while improving the energy absorption using alternative ways. To achieve this purpose, system of impact energy absorption must be developed based on principle of smart

---

Tadaharu Adachi

Department of Mechanical Engineering, Toyohashi University of Technology, Toyohashi, Japan, e-mail: adachi@mech.tut.ac.jp

structure. The main concept of the smart structure is an active control of absorption and reducing structure stiffness only when an impact occurs.

In a previous studies, the author has investigated the effect of a transverse impact on static post-buckling [6, 7] and dynamic post-buckling [8, 9] of a column to control energy absorption by experiment and finite element method (FEM). In this paper, the effect of transverse impact on the dynamic post-buckling of a column under axial impact loading was summarized. Especially effect of transverse-impact timing on energy absorption was discussed. Generating column buckling by applying an axial impact and generating beam bending by applying a transverse impact have been reported in several studies [10-13]. However, energy absorption of axially-impacted beam controlled by transverse impact has not been investigated except the author.

## 2 Concept of Energy-Absorption Control

The principle idea of this study is illustrated in Fig. 1. In the conventional

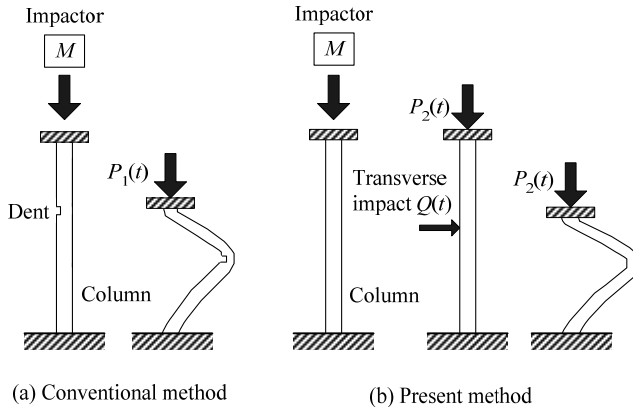


**Fig. 1** Concept of absorption by applying transverse impact

method as shown in Fig. 1(a), the stiffness of a column is reduced beforehand by adding imperfections such as a dent. When impactor  $M$  collides with the column, the structure collapses easily due to the dent, and the impact energy absorption increases. In this study, a transverse impact load  $Q(t)$  is applied to a column without an imperfection during an axial impact load  $P_2(t)$  caused by the collision of impactor  $M$ , as shown in Fig. 1(b). The transverse impact load  $Q(t)$  leads to dynamic buckling of the column and energy absorption of the column is improved without reduction of static stiffness and strength caused by imperfection.

### 3 Experiment

Based on the concept, the experimental apparatus was set up as shown in Fig. 2. First, an axial impactor was dropped onto a specimen. The axial impactor

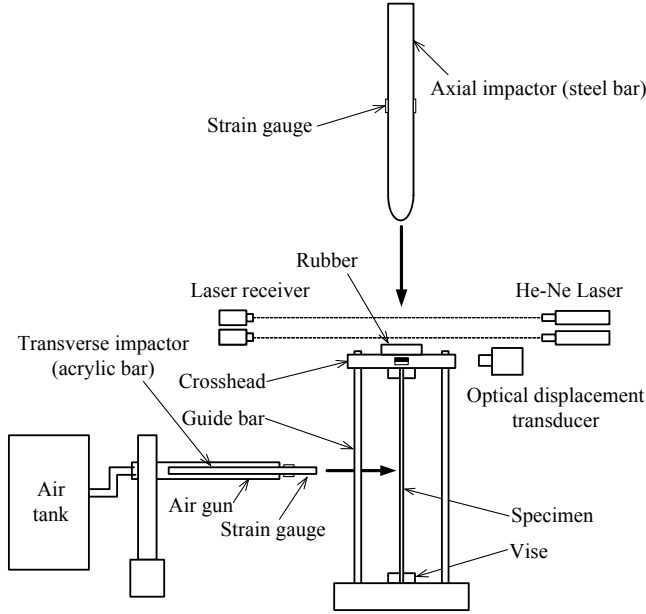


**Fig. 2** Experimental apparatus

was a steel bar with a diameter of  $40\text{mm}$  and a length of  $750\text{mm}$ . During the axial impact, a transverse impactor launched from an air gun collided with the specimen. The transverse impactor was an acrylic bar with a diameter of  $10\text{mm}$  and a length of  $600\text{mm}$ . The specimen was clamped  $30\text{mm}$  from both ends by steel vices. The crosshead could slide smoothly in vertical direction along four guide bars to compress the specimen axially. A rubber plate of  $20\text{mm}$  in thickness was set on the crosshead to prevent the axial impactor from rebounding.

The axial impact load  $P(t)$  applied to the specimen by collision with the steel bar on the crosshead can be calculated from the longitudinal strain history at the middle point of the steel bar based on the one-dimensional elastodynamics theory [14]. The strain history was measured with semiconductor gauges (Kyowa, KSP-2-120-E4). The displacement of the crosshead measured by an optical displacement transducer (Zimmer, Model 100B) was assumed to be equal to the axial displacement  $u(t)$  at the top end of the specimen.

The transverse impact load  $Q(t)$  was measured with strain gauges (Ky-

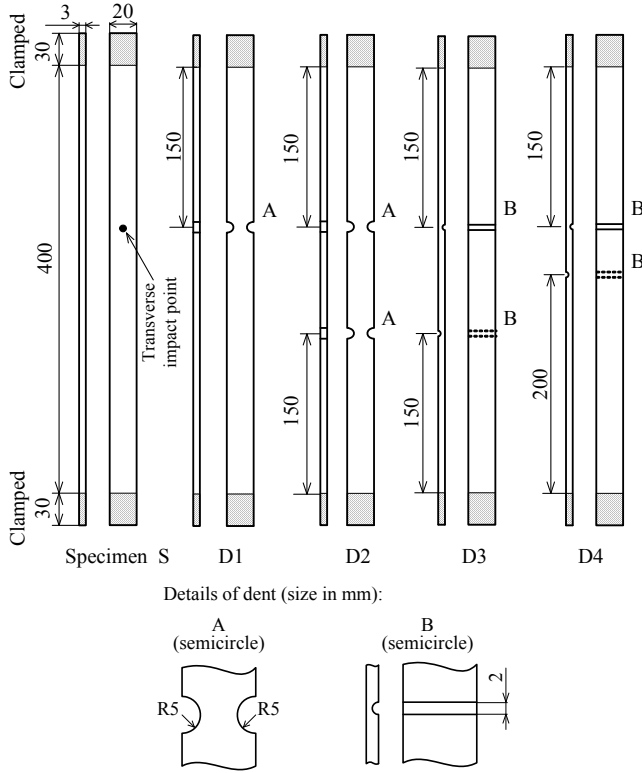


**Fig. 3** Specimens

owa, KFG-2-120-C1-23) located at 50 mm from the impacted tip of the transverse impactor. The axial impact velocity  $v_A$  and transverse impact velocity  $v_T$  were evaluated from the passing time interval between two He-Ne laser beams just before the collision with the specimen.

The specimens and the experimental conditions related to the transverse impact are shown in Fig. 3 and Table 1. Specimen  $S$  was a straight column with a length of 400 mm and a thickness of 3 mm. Specimen  $S$  was subjected to a transverse impact during an axial impact as shown in Fig. 1(b). Another test where specimen  $S$  was only applied with an axial impact was also conducted. The two tests with and without a transverse impact was distinguished as test  $S - T$  and test  $S - 0$ . Tests of the conventional method shown in Fig. 1(a) were also carried out using specimens with dents. Specimens  $D_1$  to  $D_4$  were straight columns with one or two semi-cylindrical dents, which were 2 mm and 10 mm in diameter, to easily generate buckling when applied by an axial impact only. The dents were located such that the column would buckle

easily. All specimens were made of aluminum alloy (JIS A6063). The Young's modulus and the yield stress were  $70GPa$  and  $180MPa$ , respectively. The combinations of the specimens and the experimental conditions are called the test types given in Table 1 hereafter. The axial impact velocities  $v_A$  were

Specimen	Test type	Transverse impact
$S$	$S - 0$	No
$S$	$S - T$	Applied
$D_1$	$D_1 - 0$	No
$D_2$	$D_2 - 0$	No
$D_3$	$D_3 - 0$	No
$D_4$	$D_4 - 0$	No

**Table 1** Specimens and test types

$1.7m/s$ ,  $2.6m/s$ , and  $3.5m/s$ , while the transverse impact velocities  $v_T$  were  $4.8m/s$ ,  $5.3m/s$ , and  $6.3m/s$ . The transverse impactor collided at  $250mm$  from the bottom end of specimen  $S$ .

## 4 Experimental Results

Figure 4 shows the experimental results of test type  $S - T$  with  $v_A = 3.5m/s$  and  $v_T = 5.3m/s$ . In the figures, the transverse impact time  $t_T$  is defined as the time elapsed between the collision of the axial impactor and that of the transverse impactor. Here, the results with different transverse impact times are denoted. The history of the axial impact load for test  $S - 0$  was an approximate half-sine curve with a period of  $8ms$  as shown in Fig. 4(a), while the duration of the transverse load in Fig. 4(c) was much shorter and the maximum value was smaller. The transverse impact at  $t_T = 0.4ms$  reduced the axial load more significantly compared to that with other transverse impacts and that with no transverse impact ( $S - 0$ ), as shown in Fig. 4(a). As  $t_T$  became longer, the axial load histories converged to the result of type  $S - 0$ . On the other hand, the axial displacement at the top of the specimen for the transverse impact at  $t_T = 0.4ms$  was the largest out of the results in Fig. 4(b).

From Figs. 4(a) and 4(c), the axial load-displacement curves were evaluated as shown in Fig. 4(d). The curves stood rapidly just after the axial impact, although the curves of  $S - T(t_T = 0.4ms)$  has a flatter slope due to the short  $t_T$ . After the buckling, the curve decreased gradually during the post-buckling process as the displacement increased. The transverse impact was confirmed to cause lower peaks and horizontally longer curves, which were irreversible. This means external work by the axial impact was lost by the post-buckling behavior of the specimen, that is, the energy absorption. Therefore, the absorbed energy  $E_{ab}$  of a specimen defined as the lost exter-

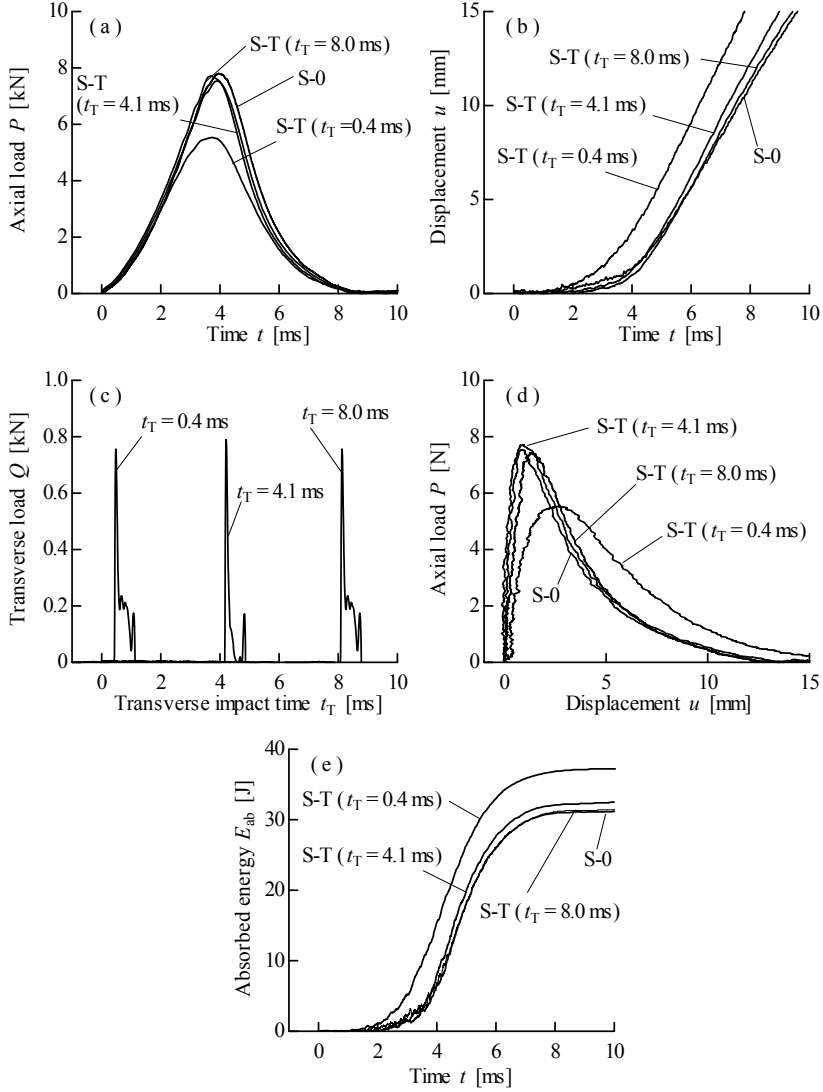


**Fig. 4** Experimental results for test type  $S-T$ : Axial impact velocity  $v_A = 3.5\text{ m/s}$ ; transverse impact velocity  $v_T = 5.3\text{ m/s}$

nal work by the axial impact, can be evaluated from the envelope area of the  $P-u$  curve.

Figure 4(e) shows the histories of energy absorption  $E_{ab}$ . All tests show different  $E_{ab}$  histories after buckling. The total  $E_{ab}$  for  $t_T = 0.4\text{ ms}$  had the highest value. The transverse impact contributes to improving the energy

absorption significantly. The transverse impact instantaneously reduced the column stiffness and made the specimen more ready to absorb higher energy. The effect was observed to be strongly dependent on the transverse impact time regardless of the transverse impact velocity.

Figure 5 shows the experimental results of tests  $S-0$ ,  $D_1$ ,  $D_2$ ,  $D_3$  and  $D_4$

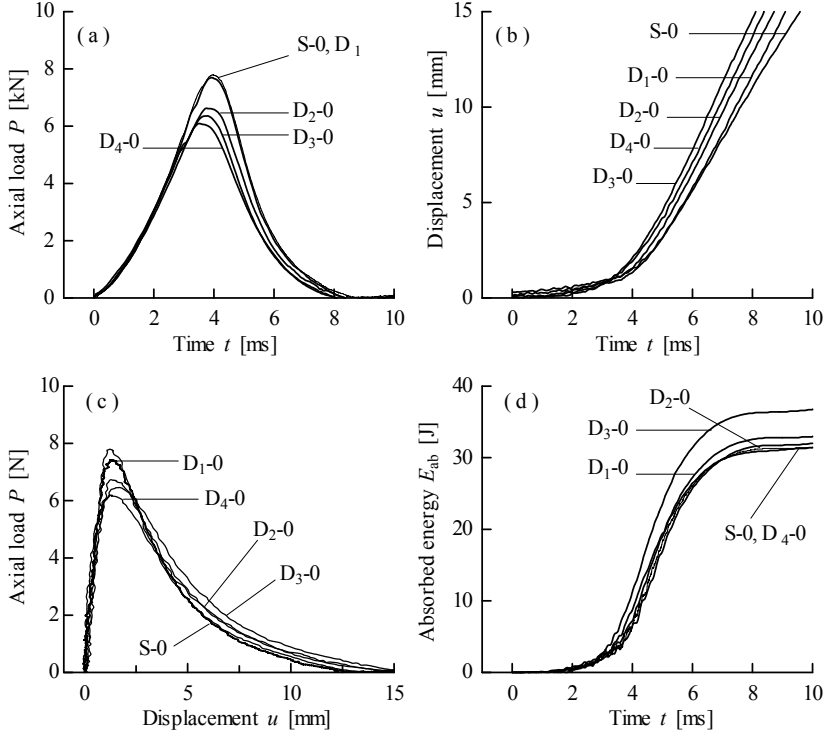


**Fig. 5** Experimental results for test types  $D_1-0$  to  $D_4-0$ : Axial impact velocity  $v_A = 3.5m/s$

(with no transverse impact) to clarify the effect of the dent on the specimen. In Fig. 5(a), each axial load was applied for approximately  $8ms$ . The axial impact loads reached the highest values for tests  $S-0$  and  $D_1-0$  and the lowest one for test  $D_4-0$ . As shown in Fig. 5(b), the axial displacement for test type  $D_3-0$  was the largest. The  $P-u$  curves are shown in Fig. 5(c). Different from the  $P-u$  curve of the tests with a transverse impact, the  $P-u$  curves for the dented specimens had the same shape as the one of test  $S-0$ , even though the peaks were lower and the displacements were horizontally longer. Figure 5(d) shows that the total energy absorption of test  $D_3-0$  was the largest compared to the other tests. As expected, these

results denoted that the existence of dents on the specimen affects increasing the energy absorption.

## 5 Discussion

In the previous section, it is described that the transverse impact time  $t_T$  strongly influenced the energy absorption. Here, the effect of  $t_T$  on absorbed energy  $E_{ab}$  and maximum value of the axial load  $P_{max}$  were considered in detail. The results for the axial impact velocity  $v_A$  at  $3.5\text{m/s}$  are shown in Fig. 6. In this figure, the efficiency of  $E_{ab}$  is defined as the ratio of  $E_{ab}$  to

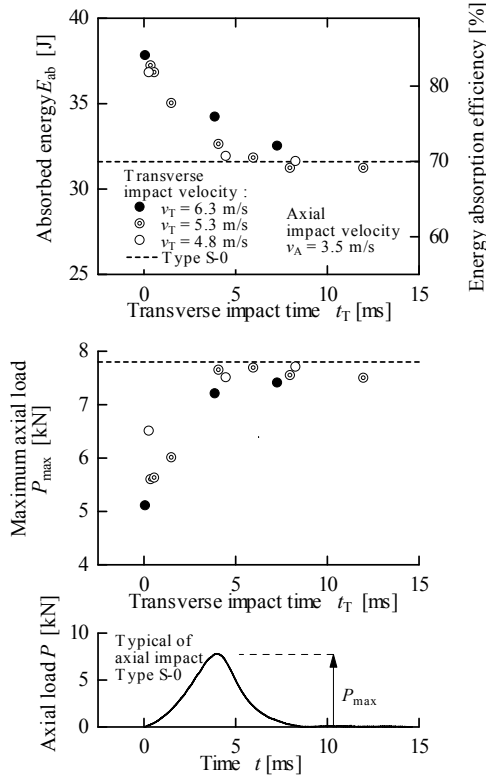


**Fig. 6** Effect of transverse impact time and transverse impact velocity

the impact energy, which is the kinetic energy of the axial impactor just before collision. In the bottom graph of Fig. 6, the history of axial load for test  $S - 0$  is shown to help understanding  $t_T$ . The  $E_{ab}$  are independent of



the transverse impact velocity  $v_T$  within the region of these experiments but they are strongly dependent on  $t_T$ . When the transverse and axial impacts were applied to the specimen simultaneously (e.g.,  $t_T \cong 0$ ), the efficiency of  $E_{ab}$  was improved by up to 18% and  $P_{max}$  was the lowest compared to the results for tests without a transverse impact. As the transverse impact time  $t_T$  became longer,  $P_{max}$  increased and  $E_{ab}$  decreased. The transverse impact had no influence on the improvement of energy absorption when it was applied after the axial impact load reached its maximum value. This was because at that time the specimen had already buckled and deformed largely. It is considered that the instantaneous imperfection of the specimen caused by the transverse impact is more effective to induce buckling at the stage of small specimen deformation. Therefore, the energy absorption was improved much more efficiently when the transverse impact was applied simultaneously with the axial impact. Similar results were obtained for different  $v_A$  and  $v_T$ .

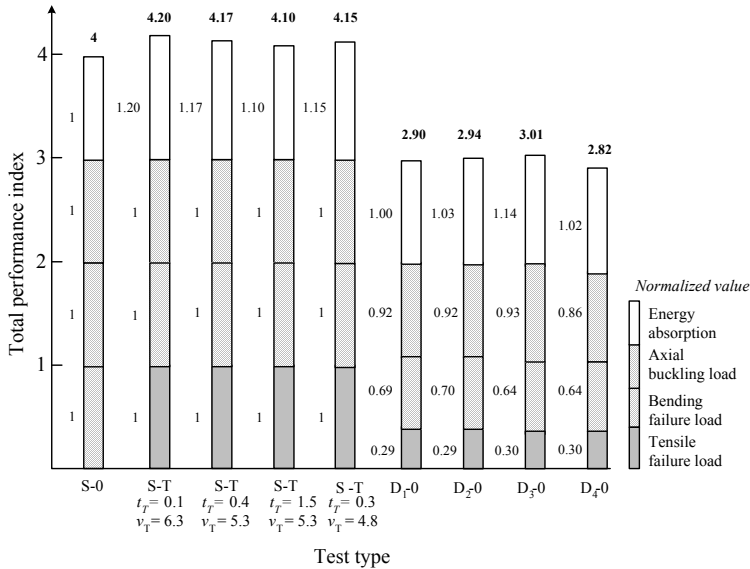


Fig. 7 Summary of energy absorption and static properties for each method

## 6 Summary

An overall comparison between the present method using a transverse impact and the conventional method using dents is summarized as a bar graph in Fig. 7. In this figure, the performance indexes are the structural properties

normalized by the values of specimen  $S - 0$  as the standards. The energy absorption for the transversely impacted specimens ( $S - T$ ) were a little larger than that of the dented specimens ( $D_1 - 0$  to  $D_4 - 0$ ) and much larger than those of test type  $S - 0$ . The transverse impact and the dent methods effectively increased the capabilities of the energy absorption. The dented specimens ( $D_1 - 0$  to  $D_4 - 0$ ) had lower buckling and failure loads than the straight specimen  $S - 0$ . Since these static properties are dependent on the shape of the specimen, the structural properties for the transversely impacted specimens ( $S - T$ ) are naturally the same as those for the straight ones ( $S - 0$ ). The present method proved to preserve the highly static properties and improve the energy absorption more effectively than the method using dents.

## References

1. Ezra AA, Fay RJ (1972) An assessment of energy absorption devices for prospective use in aircraft impact. In: Herrman G, Perrone N (ed) Dynamic response of structures. Pergamon, New York.
2. Macaulay M (1987) Introduction of impact engineering. Chapman and Hall, London.
3. Jones N (1989) Structural impact. Cambridge, Cambridge.
4. Alghamdi AAA (2001) Collapsible impact energy absorbers: an overview. Thin-Walled Struct 39:189-213.
5. Lee S, Hahn C, Rhee M, Oh JE (1993) Effect of triggering on the energy absorption capacity of axially compressed aluminum tubes. Mater & Design 20:31-40.
6. Adachi T, Tanaka T, Sastranegara A, Yamaji A, Kim SK, Yang JJ (2004) Effect of transverse impact on buckling behavior of a column under static axial force. Int J Impact Eng 30:465-475.
7. Sastranegara A, Adachi T, Yamaji A (2006) Effect of Transverse Impact on Buckling Behavior of Compressed Column. Thin-Walled Struct 44:701-707.
8. Sastranegara A, Adachi T, Yamaji A (2005) Improvement of Energy Absorption of Impacted Column due to Transverse Impact. Int J Impact Eng 31:483-496.
9. Sastranegara A, Adachi T, Yamaji A (2005) Improving Energy Absorption of Impacted Column due to Transverse Impact: Finite Element Analysis. Int J Impact Eng 32:444-460.
10. Cost TL, Jones HW (1979) Dynamic response of blast loaded prestressed flat plates. J Sound Vibration 62:111-120.
11. Zeinoddini M, Harding JE, Parke GAR (1999) Dynamic behavior of axially preloaded tubular steel members of offshore structures subjected to impact damage. Ocean Eng 26:963-978.
12. Chen FL, Yu XL (2000) Influence of axial preload on plastic failure of beams subjected to transverse dynamic load. Key Eng Mater 177-180:255-260.
13. Zeinoddini M, Parke GAR, Harding JE (2002) Axially preloaded steel tubes subjected to lateral impacts: an experimental study. Int J Impact Eng 27:669-690.
14. Adachi T, Sakanoue K, Ujihashi S, Matsumoto H (1991) Damage Evaluation of CFRP Laminates Due to Iterative Impact. Trans JSME (Series A) 57:569-575 (in Japanese).